Optimization of sputtered ZnO transparent conductive seed layer for flexible ZnO-nanorod-based devices

Petr Novák[1], Joe Briscoe[2], Tomáš Kozák[3], Martin Kormunda[4], Marie Netrvalová[1], Štěpánka Bachratá[1]

E-mail: petrnov@ntc.zcu.cz, phone: +420 377 634 773

[1]New Technologies – Research Centre, University of West Bohemia, Univerzitní 8, 306 14 Plzeň, Czech Republic

[2]School of Engineering and Material Science, Queen Mary University of London, UK

[3]Department of Physics and NTIS – European Centre of Excellence, University of West Bohemia, Czech Republic

[4] University of J.E. Purkyne in Ústí nad Labem, Faculty of Science, Department of Physics, České mládeže 8, 40096 Ustí nad Labem, Czech Republic

Abstract

The fabrication of inorganic transparent conductive oxide films on polymer substrates has been of increasing interest due to their potential applications in the field of flexible electronics. The subject of the present work is replacing the preferably-used indium tin oxide films by an aluminium zinc oxide (AZO) film in ZnO-nanorod-based devices, combining the role of the seed layer for nanorod growth with a sheet resistance lower than 100 Ω/sq. The investigated AZO films with thickness up to 300 nm were deposited on 150 μm thick polyethylene terephthalate substrates by (i) radio-frequency magnetron sputtering from a ZnO/Al_2O_3 target and (ii) co-sputtering from ZnO and Al targets in an argon atmosphere. AZO films with good transparency and thickness of 160 nm and sheet resistance lower than 100 Ω/sq were prepared by co-sputtering. It was found that co-sputtering leads to lower film resistivity due to better activation of Al atoms in the AZO film. ZnO nanorod growth was demonstrated on both types of film, and the co-sputtered AZO films were covered by a pure (undoped) ZnO film to improve the ZnO nanorod morphology.

Keywords: flexible substrate; ZnO nanorods; transparent conductive oxide; AZO; seed layer; magnetron sputtering

1. Introduction

Transparent conductive oxides (TCOs) are a class of material that combines high optical transmittance in the visible spectrum with a resistivity below 10^{-3} Ωcm. Indium tin oxide (ITO) and Al-doped zinc oxide (AZO) thin films are the most used TCOs, which are widely applied as transparent electrodes for various applications such as liquid crystal displays, organic light emitting diodes and thin film solar cells. AZO films are considered a cheap and non-toxic alternative to ITO, but it is more difficult to achieve similar values of resistivity.

Fabrication of inorganic TCOs on polymer substrates has been of increasing interest due to their potential applications in the field of flexible electronics. Nevertheless, the brittleness of inorganic thin films often results in a failure of the flexible electronic devices due to strains formed during stretching, folding or bending. The higher the film thickness, the lower is the strain required to initiate cracks in the film [1]. Thus, achieving the appropriate characteristics at the lowest possible film thickness is very important for their use in the field of flexible devices. However, lower TCO film thickness h results in higher sheet resistance R_s according to relation $R_s = \rho/h$, where ρ is the resistivity of the film. Values of R_s for specific resistivities are shown as lines in Fig. 1. The grey area in the graph denotes the suitable sheet resistance of TCO films, which should be lower than 100 Ω/sq. This means that the maximum permissible resistivity of a film with thickness 100nm is 10^{-3} Ωcm. Sheet resistance evaluated from the values published by several authors [2-7] are also included. The white and red symbols denote films prepared without heating, and at temperatures higher than 250°C,

respectively. These results illustrate the difficulty of ensuring suitable sheet resistance of low-thickness films if temperature-sensitive substrates are used.

The subject of the present work is replacing the preferably-used ITO film by an AZO film in ZnO-nanorod-based devices. These devices usually include a 100 nm-thick ITO layer as TCO and a ZnO film as a seed layer for nanorod growth [8-11]. Our main aim is to combine the role of the seed layer for nanorod growth with a sheet resistance lower than 100 Ω/sq in a single ZnO-based thin film.

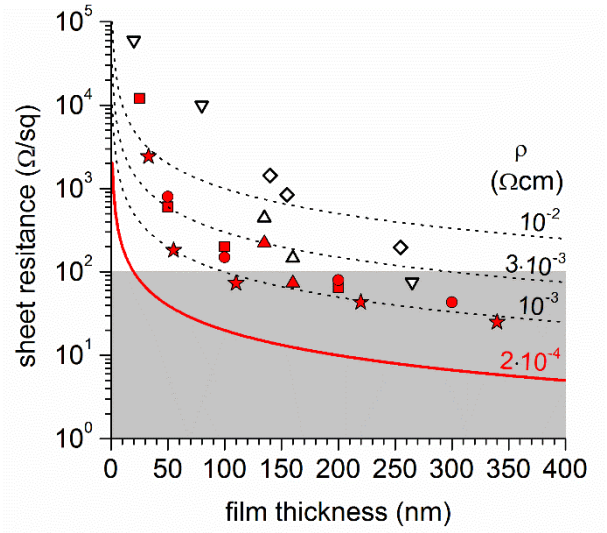

Fig. 1: Calculated sheet resistance as a function of ZnO:Al film thickness at resistivity $2x10^{-4}$, 10^{-3}, $3x10^{-3}$ and 10^{-2} Ωcm. The symbols denote the specific values taken from Li et al. [2] (circle), Bikowski et al. [3] (stars), Lee et al. [4] (triangles up), Rahmane et al. [5] (triangles down), Seo et al. [6](squares) and Hao et al. [7] (diamonds). The white and red symbols denote films prepared without heating and at temperatures of 250°C and higher, respectively. Suitable sheet resistance is lower than 100 Ω/sq (grey area). The lines denotes the sheet resistance for specific value of film resistivity.

2. Experimental setup

In this study all deposition was performed in a BOC Edwards TF 600 coating system, which is equipped with two magnetrons for targets with a radius of 76.2mm. One magnetron is connected to a radio-frequency (RF) power supply and the second is connected to a DC power supply. The investigated films were prepared by two methods: (i) RF sputtering from a ceramic ZnO/Al_2O_3 (98 wt%/2 wt%) target in an argon atmosphere and (ii) co-sputtering in an argon atmosphere from pure ceramic ZnO and Al target attached to RF and DC magnetrons, respectively. The Al content in the films prepared by co-sputtering was influenced by the DC power which was varied from 4 to 15 W. Such power range should provide an Al concentration of close to the Al concentration in ZnO/Al_2O_3 target and solubility limit of Al in ZnO (1.8 at%) [12]. All others deposition parameters were the same in both processes. The RF power was set to 300 W to minimize the influence between RF and DC magnetrons. The films were deposited on polyethylene terephthalate (PET) and Corning glass substrates. The substrate holder, heated at 100°C, was at floating potential. The substrate holder was rotated during deposition to ensure thickness homogeneity. The pressure of the Ar atmosphere was kept at 0.68 Pa by an Ar flow of 6 sccm.

The chemical surface composition of the coatings deposited on glass was studied by X-ray photoelectron spectroscopy (XPS). The XPS system (SPECS components XR50, Phoibos 100) with a base pressure below $5x10^{-7}$ Pa was used. The surface charge was corrected by setting the aliphatic carbon in C 1s peak to 284.5 eV. In the measurement, a Mg X-ray source and an Al X-ray source at 12 kV and 200 W were used without monochromators. The surface composition was calculated from XPS spectra using the standard relative sensitivity factors (RSF) from CasaXPS for the Al anode as follows C 1s (1), O 1s (2.93), Zn 3p (2.83) and Al 2s (0.753) .

The film resistivity, Hall mobility and carrier concentration were measured on square samples (8x8 mm^2) at room temperature by the Van der Pauw method using a Hall Measurement System (MMR Technologies). The surface morphology was observed using scanning electron microscopy (SEM) JEOL JSM 7600F at an operating voltage of 15 kV. ZnO nanorod morphology was studied using an FEI Inspect-F scanning electron microscope at an operating voltage of 20 kV. For the optical studies UV-Vis spectrophotometry measurements of the films were made using double-beam UV-Vis spectrophotometer Specord 210 (AnalyticJena AG) over the spectral range 190-1100 nm. Normal transmission data were obtained from films deposited on corning glass.

Many techniques are available for the growth of ZnO nanorods, generally based on the decomposition of a zinc salt in aqueous solution in the presence of an amine, such as hexamethylenetetramine (HMT) [13], potentially with additives such as ammonium hydroxide [14], and/or PEI [15]. In addition, it is also possible to dope the nanorods during growth, for example with Al, to make AZO nanorods [16]. In this study, for simplicity, a basic ZnO nanorod synthesis was used to demonstrate the principle, where the AZO-coated PET substrates were immersed face-down in an equimolar solution of 25 mM HMT and zinc nitrate and heated to 90°C for 24h [17].

3. Results

AZO films with thickness from 30 to 300 nm were first deposited from the ceramic ZnO/Al_2O_3 target. The obtained values of the film resistivity as a function of the film thickness are displayed in Fig. 2. The grey area denotes the values resulting in a sheet resistance lower than 100 Ω/sq. The value of 2.10^{-4} Ωcm, which is often presented as the

minimal possible resistivity of AZO films [18], is marked by the solid red line. It is usually important to provide at least three requirements to deposit AZO film with this low value of resistivity by magnetron sputtering, as follows. Firstly, the substrate temperature should be high enough (more than 200°C) to ensure high quality of the polycrystalline structure. This cannot be achieved on PET substrates due to a maximum working temperature between 120 and 170 °C. Secondly, the elimination of the influence of high energy negative ions on the growing film is very important. These negative oxygen ions are formed on the target surface and accelerated by the full target potential perpendicular to the target surface [19]. The impact of high energy oxygen ions can increase the AZO film resistivity by several orders of magnitude [20]. In our case, the effect of ions is limited because the targets are not aimed directly at the centre of substrate holder, where the substrates were placed during deposition. Thirdly, the film thickness should be a few hundreds of nanometers to eliminate the influence of the thin interfacial layer on these substrate, which does not contribute to electrical conductivity [21]. This effect is reflected in the measurement of resistivity, especially if the thickness of the AZO film is less than 50 nm, as the measured data in Fig. 2. The measured data also show that a suitable resistivity was only reached at a film thickness of about 300 nm, which is too high due to the risk of crack formation. The change of other depositions parameters such as RF power and pressure or using a mixture of $Ar+O_2$ has not improved the electrical conductivity of AZO film sputtered from a composite target. Therefore, AZO films prepared by the co-sputtering method were investigated.

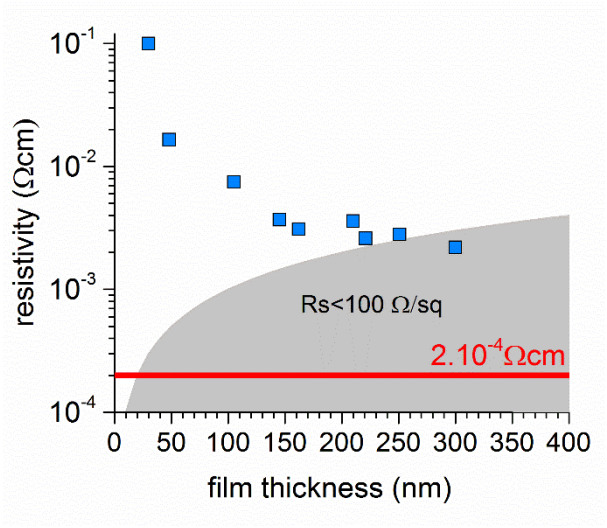

Fig. 2: Resistivity of AZO films deposited from a ZnO/Al_2O_3 target as a function of film thickness. The grey area denotes where the resistivity ensures a sheet resistance lower than 100 Ω/sq. The reported minimal possible resistivity of AZO films 2.10^{-4} Ωcm is marked by the straight solid red line.

Films with thicknesses of approximately 150 nm and 220 nm were prepared by co-sputtering from ZnO and Al targets in Ar. The values of resistivity as a function of DC power are shown in Fig. 3. For comparison, the resistivity of the films with similar thickness sputtered from a ZnO/Al_2O_3 target are marked by the blue lines. It is evident that co-sputtering allows AZO films to be deposited with resistivity up to three times lower. Moreover, the obtained data confirms that the higher film thickness results in lower resistivity. Unfortunately, some of the deposited films become less transparent, especially if

the DC-power is more than 8 W, as shown in Fig. 4. The transmittance of the AZO film prepared from the ZnO/Al_2O_3 target is also included. Nevertheless, the film prepared by co-sputtering at DC-power of 8 W (marked by the letter *a)* exhibit lower resistivity (Fig. 3) and the same transparency (Fig. 4) as the film sputtered from a ZnO/Al_2O_3 target. The adequately transparent AZO films exhibit lower value of resistivity (1.4×10^{-3} Ωcm) in comparison with the best resistivities (2.0×10^{-3} Ωcm) of the AZO films of similar thickness prepared at low temperature reported by Lee [4] and Rahmani [5]. This means that there is a process window allowing a transparent thin film with lower resistivity compared to the film sputtered from a ZnO/Al_2O_3 target to be prepared, but it is necessary to pay more attention to improving the control of the co-sputtering process. Results denoted by (a) and (b) obtained from the film prepare at P_{DC} = 8 W are slightly different. We assume that the oxygen sputtered from ZnO target can react with aluminium and partly covers the Al target surface. Aluminium oxide exhibits a much lower sputtering yield and thus fewer Al atoms are sputtered from the more oxidized Al target. This is a similar effect to the well-known target poisoning during reactive magnetron sputtering. The less transparent films probably exhibit more Al atoms due to the less poisoned target during deposition. This idea is supported by the difference of the average DC bias voltage -249 V and -232 V at the same DC power (8 W). A higher negative voltage corresponds to a less oxidized target and thus higher concentration of Al in the less transparent film as confirm XPS data in table 1. Accurate determination of the Al concentration would require precise control of the discharge voltage and power on the DC magnetron.

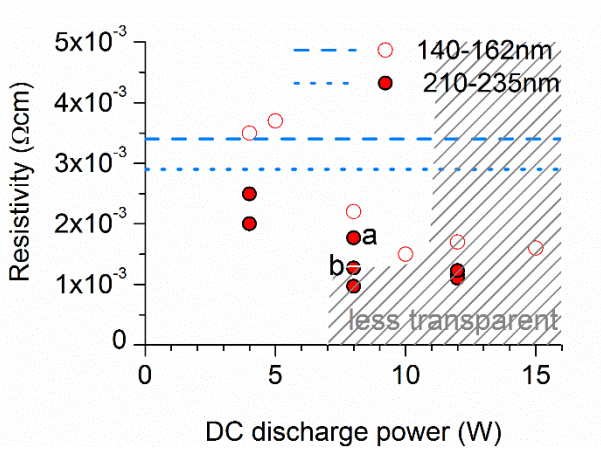

Fig. 3: The resistivity of the films prepared by co-sputtering in argon at different DC discharge powers. The less-transparent films are included in grey-hatched area. The letters (a) and (b) denote the films prepared at the same DC power, which exhibit slightly different transmittance and resistivity, see Fig 4.

The resulting sheet resistance of all prepared films are summarized in Fig. 5. Values of R_s for specific resistivities are shown as lines. Suitable values are reached at a film thickness of about 150 nm and the sheet resistance of the film with thickness about 220 nm is ~50 Ω/sq.

If high transparency is necessary, the sheet resistance is still less than 80 Ω/sq. In comparison, a film thickness of 300 nm is needed when sputtering from a ZnO/Al_2O_3 target as discussed above.

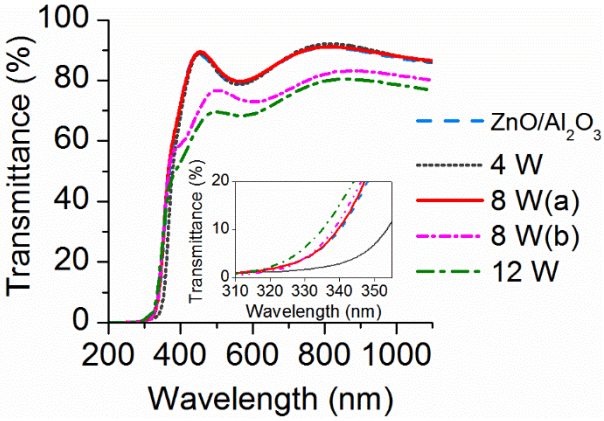

Fig. 4: The transmittance spectra of the films with thickness ~220 nm on the glass substrate, prepared under different deposition conditions. The inset shows transmittance close to the absorption edge. The letters (a) and (b) denote the films prepared at the same DC power, which exhibits slightly different transmittance and resistivity, see Fig 3.

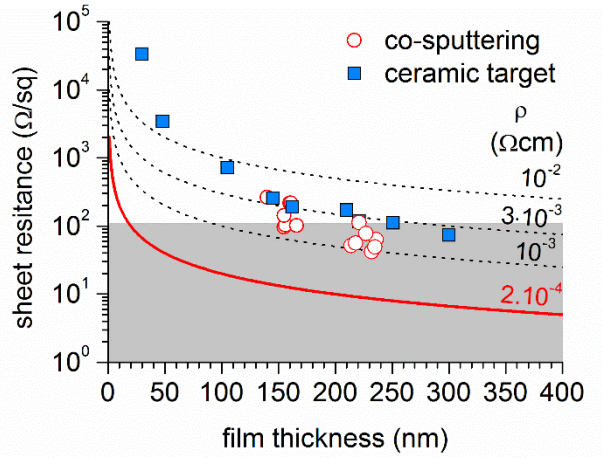

Fig. 5: Sheet resistance of the sputtered films as a function of the thickness. The lines denote the sheet resistance for specific values of film resistivity.

The XPS study of AZO samples prepared by both techniques detected only the expected elements Zn, O, C and Al. The binding energies of the photoelectron peaks taken on investigated samples were practically identical. All samples exhibited practically identical binding energies for the elements, therefore only the results from selected coating example are presented in Fig. 6 and 7. The survey spectra show multiple loss energy peaks, resulting from non-elastic electron scattering processes, as it also reported in literature [22] and characteristic Auger peak Zn LMM. A simple way to identified peaks not related to photoelectrons is to compare survey spectra taken with Al and Mg anodes (different photo energies), see in Fig. 6. The detail analyses detected systematic difference in area/RSF ratio between Zn 2p, Zn 3s and Zn 3p photoelectron peaks, see in Fig 7a. and 7b, where information from approx. top 3 nm and approx. 7 nm is kept, respectively. There is relatively less zinc in the top 3 nm area than the top 7 nm area, which indicates presence of the carbon above the AZO coating, therefore we conclude that the carbon is not part of the AZO film itself. The Al/(Al+Zn) ratio were used to compare the AZO films, see table 1.

The Zn 2p single peak character in each spin state and position of Zn LMM peak indicates a presence of ZnO, see Fig. 6. The peak position located at around 1021 eV is assigned to the Zn $2p_{3/2}$, confirming that the zinc exists in the +2 oxidation state in the ZnO host lattice [22, 23]. Al 2s was detected at about 118.3 eV as it is typical for Al_2O_3 and AlOH [23] but the concentration of Al is very low for precision chemical state detection, see Fig. 7b. Moreover the Al 2s peak is influenced by a loss peak from Zn 3p and the Al 2p peak is influenced by a satellite peak from Zn 3p due to the non-monochromatic X-ray source. The O 1s spectrum in Fig. 7c show the existence of two components O_1 and O_2 positioned at around 530 eV and 531.5 eV corresponding to O^{2-} and –OH groups on the surface, respectively [22, 24]. The detail analysis of the O 1s spectra showed a small but systematic decrease in the O_1/O_2 ratio at higher P_{DC} on co-sputtered AZO films, see Table 1. Composite target deposited films had an even smaller ratio.

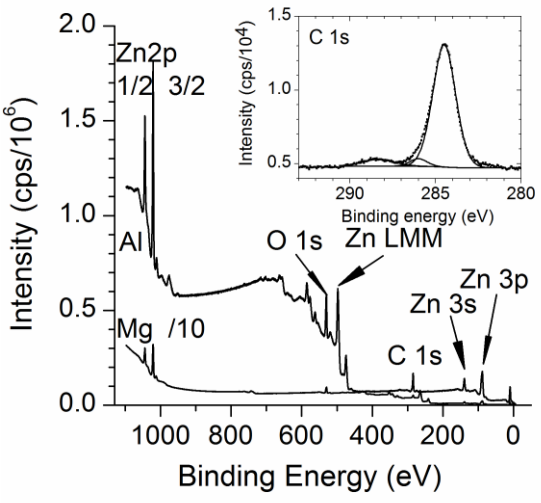

Fig. 6 Survey XPS spectra acquired with Al anode and Mg anode (10 times attenuated for readability) with inset showing calibrated C 1s photoelectron peak of the AZO films deposited from ZnO/Al_2O_3 target.

The Hall mobility and carrier concentration of the selected films are listed in Table 1. The co-sputtered films exhibit a higher carrier concentration and thus lower resistivity, although the Al concentration is lower in comparison with the film deposited from the ZnO/Al_2O_3 target. This means that more Al atoms are acting as donors if the co-sputtering regime is used. This could be related to the lower probability of forming secondary phases such as Al_2O_3, due to lower amounts of oxygen in the growing film. The formation of these phase can lead to the electrical deactivation of the dopant [18]

.

Table 1. The deposition method, applied DC power P_{DC}, thickness *h*, Al/(Al+Zn) and O_1/O_2 ratios obtained by XPS, resistivity **ρ**, carrier concentration *n*, Hall mobility **μ** and sheet resistance R_s

Deposition method	**P_{DC} (W)**	**h (nm)**	**Al/(Al+Zn) (%)**	**O_1/O_2**	**ρ (10^{-3}Ω .cm)**	**n ($10^{20}cm^{-3}$)**	**μ (cm^2/Vs)**	**R_s (Ω/sq)**
ZnO/Al_2O_3	0	162	4.19	1.38	3.53	1.97	9.0	218
	0	221	4.24	1.39	2.68	2.09	11.1	121
Co-sputtering	4	158	0.71	1.76	3.59	1.06	16.3	223
	8	161	2.25	1.75	2.50	2.05	12.2	161
	12	155	7.91	1.40	1.88	2.92	11.3	113
	4	221	1.24	1.75	2.49	1.30	19.3	113
	8(a)	227	1.79	1.62	1.77	2.54	13.9	78
	8(b)	214	5.10	-	1.27	3.82	12.9	59
	12	218	5.72	1.59	1.18	4.21	12.6	54

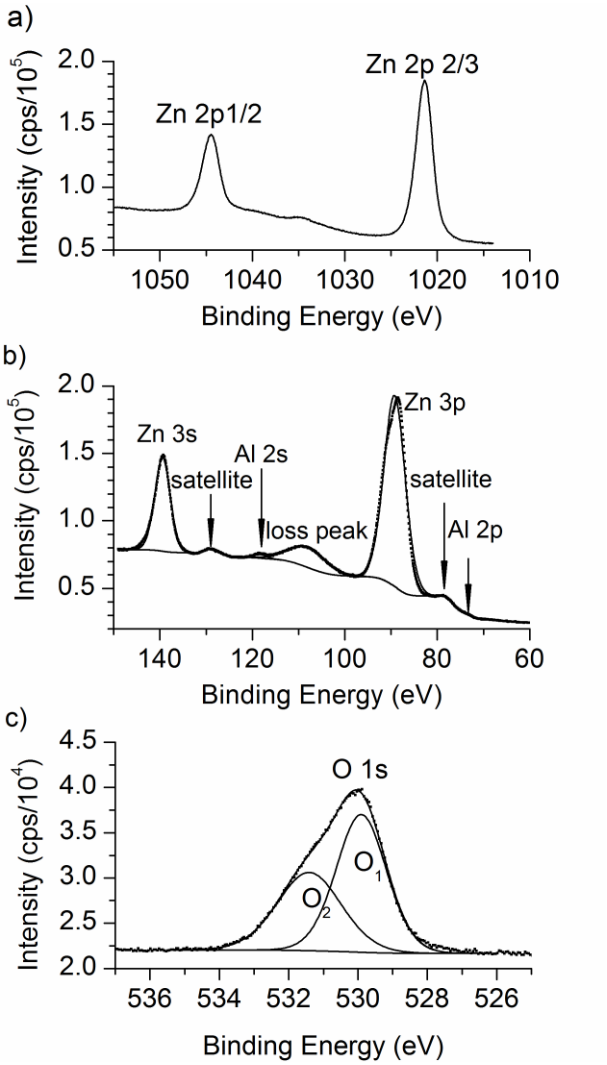

Fig. 7: (a) High resolution XPS spectra of Zn 2p, (b) detail spectra of Al region and (c) high resolution spectra of O 1s peak of the AZO films deposited from ZnO/Al_2O_3 target

The films deposited on PET substrate from a ZnO/Al_2O_3 target with thickness of 145 nm and 210 nm were tested as a seed layer for growth of ZnO nanorods. Prior to nanorods growth, the surface morphology was observed by SEM, see Fig. 8a and 8b. Both surfaces are homogeneous without any voids and cracks. The morphology of the thicker AZO film

exhibits larger grains. The as-grown nanorods (see Fig. 9a and 9b) show a more developed structure on the thicker films resulting in longer nanorods. This likely results from a better nucleation and growth on the more developed grain structure of the thicker film.

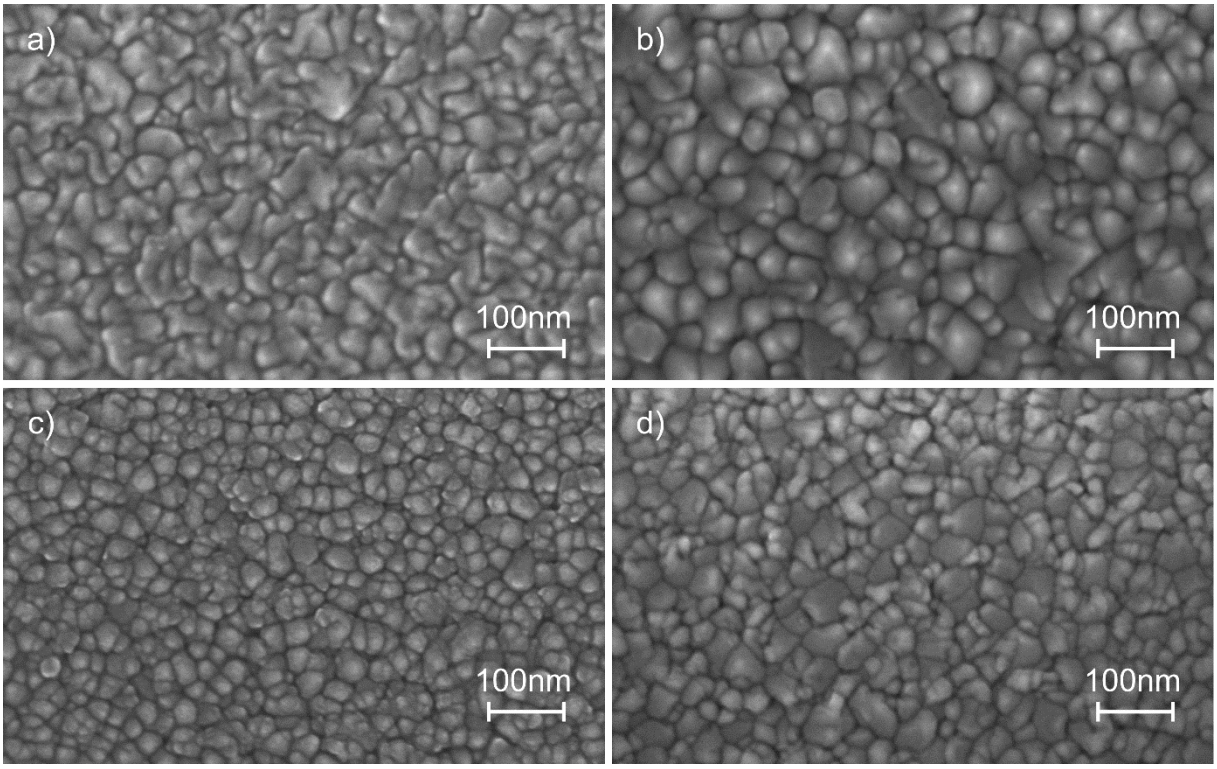

Fig. 8: Surface morphology of the films tested as a seed layer for nanorod growth. SEM micrographs were collected from AZO films prepared by sputtering from a ZnO/Al_2O_3 target with thickness (a) 145 nm and (b) 210 nm, (c) from 214 nm thick AZO film prepared by co-sputtering at DC power 8 W and (d) from AZO/ZnO film prepared by co-sputtering

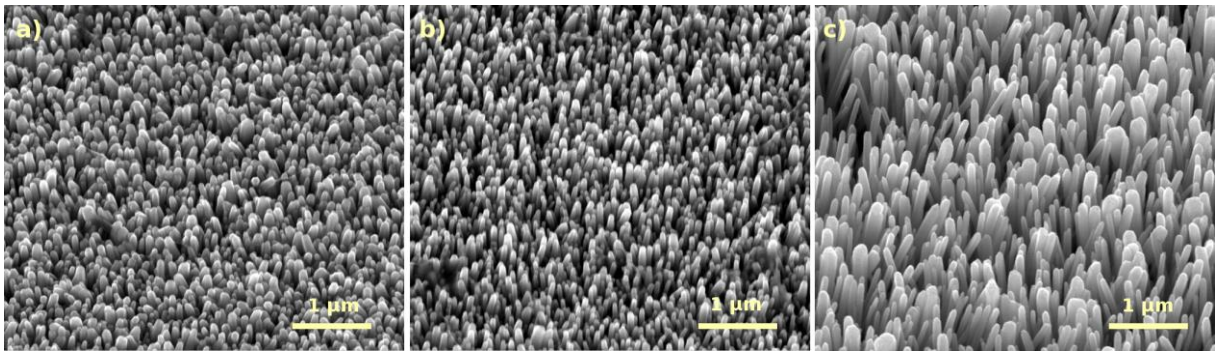

Fig. 9: SEM micrographs of ZnO nanorods grown on the AZO films prepared by sputtering from a ZnO/Al_2O_3 target with thickness (a) 145 nm and (b) 210nm and from an AZO/ZnO film prepared by co-sputtering (c).

The surface morphology of the AZO film prepared by co-sputtering is shown in Fig. 8c. If co-sputtering is used, the film structure is much finer, which is not suitable for ZnO nanorod seeding [25]. Thus, the AZO films was covered by the pure ZnO to improve the seed layer ability. A 165 nm AZO film was sputtered at a DC-power of 8 W and then the DC power supply was switched off and 55 nm was deposited as pure ZnO. The surface morphology of the AZO/ZnO structure is shown in Fig. 8d and the nanorods grown on it are shown in Fig 9c. The nanorods length and width vary between 500-700 nm and 40-150 nm, respectively. The nanorods are much longer and wider than those grown on either of the films from the composite target, which may result from the larger grains of this film, but also possibly the better nucleation on the intrinsic ZnO layer which was sputtered on top of the AZO film, facilitated by the co-sputtering process. The ZnO layer was not combined with the AZO film prepared from the ZnO/Al_2O_3 target because of the need to vent the vacuum chamber and change the targets between AZO and ZnO depositions. Fabricating the AZO/ZnO film without changing the deposition system is an advantage of co-sputtering.

4. Conclusion

Transparent conductive AZO films were prepared by two methods on PET substrates at temperature of 100°C. It was found that co-sputtering enables the deposition of approximately 160 nm thick AZO films with sheet resistance below 100 Ω/sq and 220nm thick AZO films with sheet resistance below 60 Ω/sq due to more Al atoms acting as donors in comparison to films deposited from a ZnO/Al_2O_3 target, which could only produce resistance below 100 Ω/sq when 300 nm thick. Moreover, co-sputtering allows the deposition of AZO/ZnO film, which was tested as a seed layer for ZnO nanorods growth, and showed improved nanorod growth compared to films deposited from the composite target.

Acknowledgement

This research was supported by the Czech Ministry of Education, Youth and Sports projects CENTEM CZ.1.05/2.1.00/03.0088 and CENTEM PLUS LO1402. Author MK also acknowledge the assistance provided by the Research Infrastructure NanoEnviCz under Project No. LM2015073. JB acknowledges funding from Innovate UK project 101796.

Referencces:

[1] B. Ch. Mohanty, H. R. Choi, Y. M. Choi, Y. S. Cho, Thickness-dependent fracture behaviour of flexible ZnO: Al thin films, J. Phys. D 44 (2011), 025401

[2] C. Li, M. Furuta, T. Matsuda, T. Hiramatsu, H. Furuta, T. Hirao, Effects of substrate on the structural, electrical and optical properties of Al-doped ZnO films prepared by radio frequency magnetron sputtering, Thin Solid Films 517 (2009) 3265-3268

[3] A. Bikowski, M. Rengachari, M. Nie, N. Wanderka, P. Stender, G. Schmitz, K. Ellmer, Research Update: Inhomogeneous aluminium dopant distribution in magnetron sputtered ZnO:Al thin films and its influence on their electrical properties , Appl. Phys. Lett. Mater. 3 (2015) 060701

[4] M. Lee, J. Lim, J. Bang, W. Lee, J. Myoun , Effects of thickness variation on properties of ZnO:Al thin films grown by RF magnetron sputtering deposition, Applied Surface Science 255 (2008) 3195–3200

[5] S. Rahmane, M. S. Aida, M. A. Djouadi, N. Barreau, Effects of thickness variation on properties of ZnO:Al thin films grown by RF magnetron sputtering deposition, Superlattices and Microstructures 79 (2015) 148-155.

[6] K. Seo, H. Shin, J. Lee, K. Chung, H. Kim,The effects of thickness on the electrical, optical, structural and morphological properties of Al and Ga co-doped ZnO films grown by linear facing target sputtering, Vacuum 101 (2014) 250-256.

[7] X. Hao, J. Ma, D. Zhang, T. Yang, H. Ma, Y. Yang, Ch. Cheng, J. Huang, Thickness dependence of structural, optical and electrical properties of ZnO:Al films prepared on flexible substrates, Applied Surface Science 183 (2001) 137-142

[8] J. Briscoe, N. Jalali, P. Woolliams, M. Stewart, P.M. Weaver, M. Cain, S. Dunn, Measurementtechniques for piezoelectric nanogenerators, Energy Environ. Sci. 6 (2013) 3035-3045

[9] Briscoe, J.; Bilotti, E.; Dunn, S. Measured Efficiency of a ZnO Nanostructured Diode Piezoelectric Energy Harvesting Device, Applied Physics Letters 101 (**2012)** 93902.

[10] Jalali, N.; Woolliams, P.; Stewart, M.; Weaver, P. M.; Cain, M. G.; Dunn, S.; Briscoe, J. Improved Performance of P–n Junction-Based ZnO Nanogenerators through CuSCN-Passivation of ZnO Nanorods. Journal of Materials Chemistry A 2 (2014), 10945.

[11] Tong, F.; Kim, K.; Martinez, D.; Thapa, R.; Ahyi, A.; Williams, J.; Kim, D.-J.; Lee, S.; Lim, E.; Lee, K. K.; Park, M. Flexible Organic/inorganic Hybrid Solar Cells Based on Conjugated Polymer and ZnO Nanorod Array. Semiconductor Science and Technology 27, (2012), 105005.

[12] T. Minami,H. Nanto and S. Takata, Highly conductive and transparent ZnO thin films prepared by r.f. magnetron sputtering in an applied external d.c. magnetic field, Thin Solid Films 124 (1985) 43–47

[13] G.-C. Yi, C. Wang, W. Il Park, ZnO nanorods: synthesis, characterization and applications, Semiconductor Science and Technology. 20 (2005) S22-S34.

[14] A. Resmini, I.G. Tredici, C. Cantalini, L. Giancaterini, F. De Angelis, E. Rondanina, M. Patrini, D. Bajonie, U. Anselmi-Tamburini, A simple all-solution approach to the synthesis of large ZnO nanorod networks, J. Mater. Chem. A. 3 (2015) 4568-4577.

[15] M. Law, L.E. Greene, J.C. Johnson, R. Saykally, P. Yang, Nanowire dye-sensitized solar cells, Nature Materials. 4 (2005) 455-459.

[16] C. Hsu, D. Chen, Synthesis and conductivity enhancement of Al-doped ZnO nanorod array thin films, Nanotechnology. 21 (2010) 285603.

[17] Briscoe, J.; Stewart, M.; Vopson, M.; Cain, M.; Weaver, P. M.; Dunn, S. Nanostructured P-N Junctions for Kinetic-to-Electrical Energy Conversion, Advanced Energy Materials 2 (2012) 1261–1268.

[18] K. Ellmer, A. Bikowski, Intrinsic and extrinsic doping of ZnO and ZnO alloys, J. Phys. D: Appl. Phys. 49 (2016) 413002

[19] T. Welzel, K. Ellmer, The influence of the target age on laterally resolved ion distributions in reactive planar magnetron sputtering, Surface Coatings Technology 205 (2011) S294–S298.

[20] L. W. Rieth, P. H. Holloway, Influence of negative ion resputtering on ZnO: Al thin films, J. Vacuum Sci. Technol. A 22 (2004) 20-29.

[21] M. Nie, A. Bikowski, K. Ellmer, Microstructure evolution of Al-doped zinc oxide and Sn-doped indium oxide deposited by radio-frequency magnetron sputtering: A comparison, Journal of Applied Physics 117 (2015) 155301.

[22] A. Sreedhar,J. H. Kwon,J. Yi ,J. S. Gwag, Improved physical properties of Al-doped ZnO thin films deposited by unbalanced RF magnetron sputtering, Ceramics International 42 (2016) 14456–14462

[23] B. Crist, Handbook of monochromatic XPS Spectra, XPS International, 2004

[24] R. Al-Gaashani, S. Radiman, A.R. Daud, N. Tabet, Y. Al-Douri, XPS and optical studies of different morphologies of ZnO nanostructures prepared by microwave methods, Ceramics International 39 (2013) 2283-229

[25] N. T. Son, J. Noh, S. Park, Role of ZnO thin film in the vertically aligned growth of ZnO nanorodsby chemical bath deposition, Applied Surface Science 379 (2016) 440-445